Gas-Transfer Simulations with the PAR3D Numerical Model

Robert S. Bernard[1]

Abstract

The PAR3D code is a general-purpose numerical model that uses parallel processors for computing three-dimensional incompressible flow. Its modeling capabilities include turbulence, bubble plumes, and gas transfer. The present work concerns application of the model to bubble plumes in water, and the gas transfer associated therewith. PAR3D employs a *k-,* model for turbulence, a large-eddy model for gas transfer at the free surface, and a Levich (single-bubble) formula for gas transfer in the plume. The bubble diameter is used as an empirical tuning parameter in the latter formula. Computed results for velocity and gas-transfer are compared with tank-test data for bubble diffusers submerged in 10 to 33 feet (3 to 10 meters) of water.

Model Description

PAR3D is a descendent of the MAC3D code (Bernard 1995, 1998), previously developed for sequential (scalar and vector) computers at the ERDC Waterways Experiment Station. Unlike its predecessor, which was limited to fixed grids, rigid boundaries, and single processors, PAR3D incorporates deforming grids, quasi-static free-surface displacement, and multiple processors. Its modeling capabilities include turbulence (with buoyancy), transfer and transport of dissolved gas, and flow driven by bubble plumes.

PAR3D uses finite-volume discretization with curvilinear marker-and-cell (MAC) grids to solve the Reynolds-Averaged Navier-Stokes (RANS) equations for incompressible flow. The MAC designation refers to the volume-averaged evaluation of scalar quantities inside the grid cells, and the surface-averaged evaluation of normal vector components on the cell faces. Grids are constructed such that, regardless of their shape in Cartesian (*xyz*) space, they map into a rectangular grid in computational (*ijk*) space. Integer *ijk*-coordinates then serve as indices for identifying grid cells, and as coordinates for locating grid nodes in the computational space. Grids ordered in this way are generally called structured grids.

The RANS momentum equation is discretized in space with a three-point upwind approximation for advective terms, and a central-difference approximation for diffusion terms. Discretization in time is achieved using a two-level (first-order) approximation for time derivatives, with time-lagged (explicit) evaluation of advective terms, and time-advanced (implicit) evaluation of diffusion terms.

[1] Research Physicist, CEERD-HC-I, ERDC Waterways Experiment Station, Vicksburg, MS 39180-6199, Telephone 601-634-2491, E-mail BernarR@wes.army.mil

The solution scheme for the momentum equation entails a two-step procedure in which velocity increments are first computed without a pressure gradient, and then corrected by imposing a pressure gradient that enforces conservation of mass at the end of each time step. This pressure gradient is extracted from the solution of a Poisson equation for pressure, which itself is derived by combining the full RANS momentum equation with the continuity equation for incompressible flow.

Reynolds stresses (shear stresses arising from turbulence) are computed by supplementing molecular viscosity with an eddy viscosity, given by

$$\nu_T = c_\nu \frac{k^2}{\varepsilon}$$

where k is the turbulence energy (per unit mass), ε is the dissipation rate (for k), and the coefficient $c_\nu = 0.09$. The variables k and ε are obtained from a k-ε turbulence model (Launder and Spalding 1974), discussed in the Appendix, which employs separate equations for production and transport of these quantities throughout the flow. The empirical coefficients in these equations have been adjusted for improved accuracy in recirculating flow (see Appendix); and the associated production terms include contributions from shear and buoyancy, as discussed by Rodi (1980).

For computing shear stress along no-slip boundaries, the boundary-adjacent tangential velocity profile is assumed to be logarithmic, in accordance with the conventional law of the wall. Along a free surface, however, the adjacent tangential velocity is assumed to have a vanishing normal derivative, which approximates a condition of zero shear stress. To accommodate fairly coarse grids, and to allow for the likely generation of turbulence by processes occurring far from the boundaries, vanishing normal derivatives are imposed on k and ε along all physical boundaries (free or fixed) that constrain the flow.

The fluid is assumed to be mechanically incompressible, which means that its density is unaffected by changes in pressure. The density may still vary with temperature though, and the *effective* density varies with the local concentration of undissolved gas (i.e., gas bubbles) suspended in the flow. For computing the downward force imposed by gravity, the effective density is approximated by

$$\rho_{eff} \approx \rho(T)(1-\phi)$$

where $\rho(T)$ is the temperature-dependent density, and ϕ is the void ratio created by the bubbles.

Gas-Transfer Equations

For PAR3D applications involving air bubbles, the composition of the injected gas is taken to be 79 percent nitrogen and 21 percent oxygen. To facilitate gas-transfer

calculations, separate transport equations are used for each of the dissolved and undissolved gas components, making four gas-transport equations in all. In the formula for effective density, however, contributions from both of the undissolved gases are combined to yield a single value for the bubble-void ratio *N*.

The air-to-water gas-transfer process can proceed in either direction, with dissolved gas becoming undissolved gas and vice versa. When the concentration of dissolved gas exceeds the local saturation concentration adjacent to a bubble (or free surface), dissolved gas comes out of solution and enters the bubble (or ambient air). Otherwise, undissolved gas leaves the bubble (or ambient air) and goes into solution in the water.

Across any air-water interface with surface area A, the rate of mass transfer m_t into the water is given approximately by

$$m_t \approx K_L \, A \left(C_{sat} - C \right)$$

where K_L is the liquid-film transfer coefficient (expressed with dimensions of length per unit time), C is the mass concentration (mass per unit volume) of dissolved gas in the water, and C_{sat} is the mass concentration at saturation.

A separate transfer equation applies for each gas involved in the transfer process, and the formula used for K_L depends on whether the air-water interface is a free surface or a bubble surface. Along a free surface in particular, PAR3D employs a large-eddy approximation for K_L, equivalent to that of Fortesque and Pearson (1967),

$$K_L \approx 2.15 \left(\frac{D \varepsilon}{k} \right)^{1/2}$$

where D is the molecular diffusion coefficient for the dissolved gas in water. Otherwise, for bubbles, PAR3D uses a formula developed by Levich (1962),

$$K_L \approx \left(\frac{2 D w_B}{\pi d_B} \right)^{1/2}$$

where d_B is the bubble diameter, and w_B is the bubble velocity (relative to the water), approximated by

$$w_B \approx \left(w_0^2 + 2k \right)^{1/2}$$

with w_0 representing the slip velocity (rise velocity) for a single bubble. Levich's original implementation of this formula used only w_0 instead of the turbulence-dependent approximation proposed here for w_B, and the latter may represent an upper bound for effective velocity of the bubbles relative to the water. Whatever the case,

the incorporation of k into the definition for w_B produces a slight improvement in the agreement achieved between predicted and observed rates of gas transfer.
In the PAR3D implementation of the Levich formula for K_L, the bubble diameter d_B is assumed to vary with the local static pressure p via the relation,

$$d_B \approx d_0 \left(1 + \frac{p}{p_{atm}} \right)^{-1/3}$$

where p_{atm} is atmospheric pressure, and d_0 is the nominal bubble diameter at one atmosphere. This adjustment accounts for isothermal reduction in bubble volume with increasing pressure, and the resulting dependence of d_B on p implies that effective diameter gradually increases as a bubble rises toward a free surface.

For bubble diameters ranging from 0.04 to 1.0 inches (1 to 25 mm), the slip velocity w_0 varies by no more than a factor of two, with a median value of about 1 ft/sec, as discussed by Clift, Grace, and Weber (1978). Assuming that the latter value can be used by default for w_0, the nominal diameter d_0 then becomes an empirical parameter that can be used to tune K_L for the plumes generated by individual bubble diffusers. In principle, the value of d_0 should be inferred from a weighted average of inverse bubble diameter in a given plume. In practice, the appropriate (empirically determined) value of d_0 falls somewhere in the *range* of actual bubble diameters produced by a given diffuser. Whatever the case, d_0 must be determined separately for each diffuser modeled with PAR3D, and it is the only parameter used to tune the rate of gas transfer for bubble plumes.

Model Application

Laboratory experiments were conducted in a 25-ft-diameter tank to determine the flow velocities[2] and oxygen-transfer rates[3] created by a coarse-bubble diffuser in 10 to 33 ft of water. The injected gas was air, and the airflow rate was varied from 15 to 60 standard cubic feet per minute (scfm). The diffuser was placed at the center of the tank, 2 ft from the bottom, and the water was purged of dissolved oxygen prior to each of the gas-transfer experiments.

Velocity measurements were taken with an acoustic Doppler velocimeter, and then time-averaged for comparison with model predictions. Assuming the tank to be fully mixed at all times, a bulk oxygen-transfer coefficient $K_L a$ was inferred from the observed increase in dissolved-oxygen concentration with time, using the definition

[2] Unpublished velocity measurements provided by Gary P. Johnson, November 1995, U.S. Geological Survey, U.S. Department of the Interior, Urbana, IL.
[3] Unpublished gas-transfer measurements provided by Charles W. Downer, Laurin I. Yates, and Calvin Buie, Jr., September 1995, ERDC Waterways Experiment Station, Vicksburg, MS.

$$K_L a = -\frac{1}{t} ln\left(\frac{C_{eq} - C}{C_{eq} - C_{in}}\right)$$

where C is the concentration at time t, C_{in} is the initial concentration, and C_{eq} is the equilibrium concentration. The bulk coefficient $K_L a$ amounts to a volume-averaged product of the film coefficient K_L with the transfer surface area A, and it has units of inverse time. Here the transfer surface includes the bubble plume *and* the free surface.

PAR3D simulations were conducted using grids with a uniform vertical spacing of 1.0 ft, and an average radial spacing of 0.962 ft. The diffuser was represented as a cylindrical region centered on the tank axis, 2.0 ft in diameter and 1.0 ft in height, into which undissolved air was introduced at the appropriate flow rate.

In all cases, the nominal bubble diameter was set at d_0 = 0.236 inches (6.0 mm), and simulated air injection was started impulsively in the quiescent tank. The subsequent time-development of the bubble plume, the flow field, and the dissolved-gas distributions then followed the dictates of the various governing equations. For the purpose of comparing predicted and measured velocities, the model was allowed to run only until the flow reached steady state. For comparing predicted and measured oxygen-transfer rates, however, the model was allowed to continue running until the dissolved oxygen reached equilibrium.

Figure 1 shows a comparison of predicted and observed profiles of absolute velocity (velocity magnitude) for an airflow rate of 35.5 scfm in 10 ft of water. The PAR3D predictions represent steady-state values, and the experimental data are time-averaged values (taken over three-minute intervals). Vertical profiles are shown at four different radial positions (as measured from the central axis of the tank), and the relative agreement (or disagreement) achieved with experiment is typical of PAR3D predictions for bubble diffusers in general.

As a rule of thumb, PAR3D (without adjustment) seems to predict velocities locally within a factor of two or better. Moreover, these velocity predictions are fairly insensitive to factor-of-two changes in the bubble diameter, the slip velocity, and the idealized radius of the diffuser. Refinement of the computational grid spacing by a factor of two alters the predicted velocities only slightly.

Figure 2 offers a comparison of predicted and observed values for $K_L a$, plotted against diffuser airflow rate. Predicted $K_L a$ results are shown for total water depths of 11, 22, and 33 ft, while experimental data are presented for these depths, and for 31.6 ft as well. The agreement between model and experiment is very good at airflow rates of 15 and 30 scfm, but somewhat less so at 45 and 60 scfm.

The value used for the nominal bubble diameter (d_0 = 6 mm) was arrived at by trial-and-error computations with PAR3D. Factor-of-two decreases (or increases) in d_0 will shift the predicted $K_L a$ curves up (or down), roughly by a factor of three, without

significantly changing the shapes of the curves or the relative dependence on depth that is evident in Figure 2.

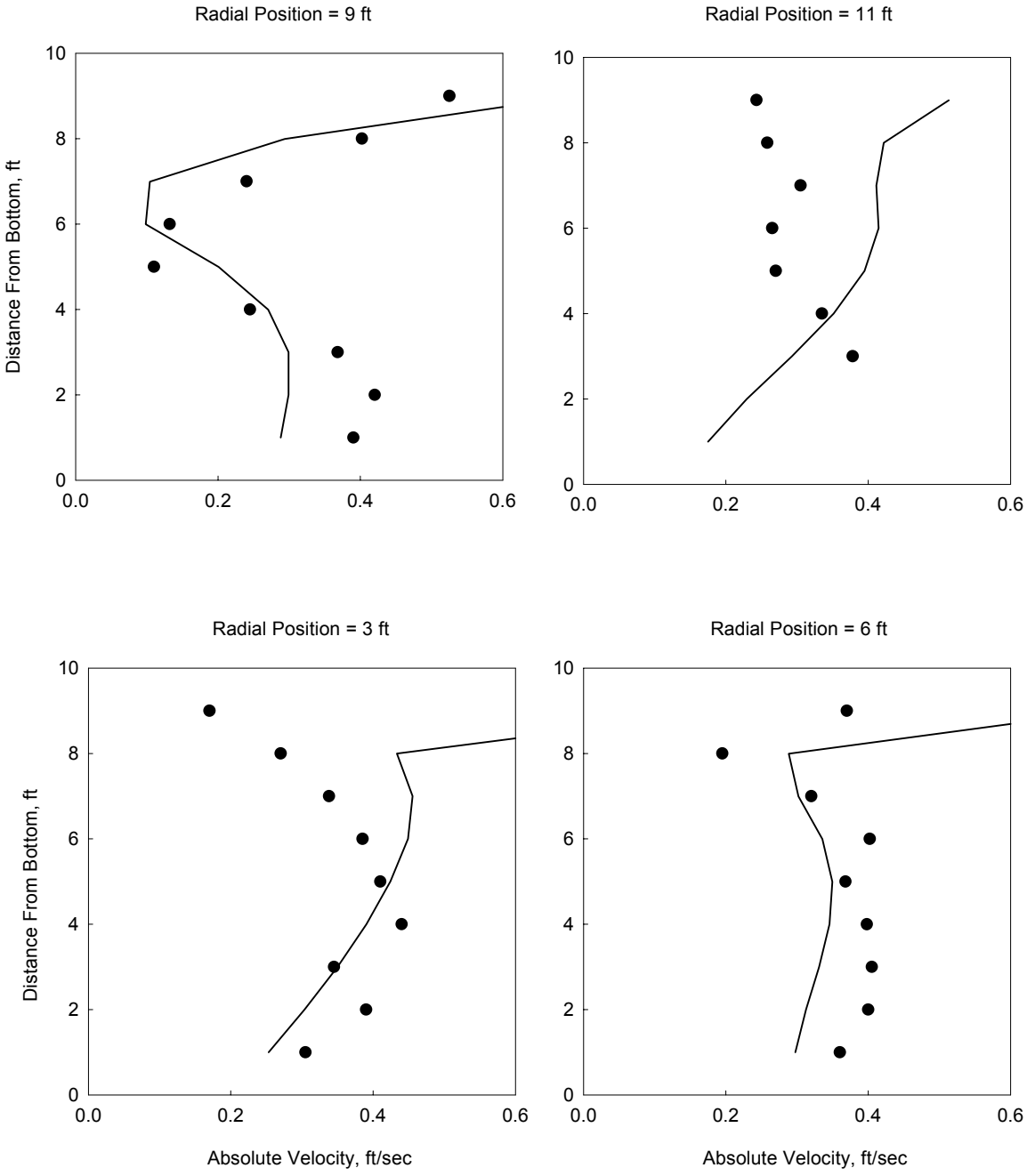

Figure 1. Predicted (—) and observed (•) velocity profiles for coarse-bubble diffuser submerged in 10 ft of water in 25-ft-diameter tank

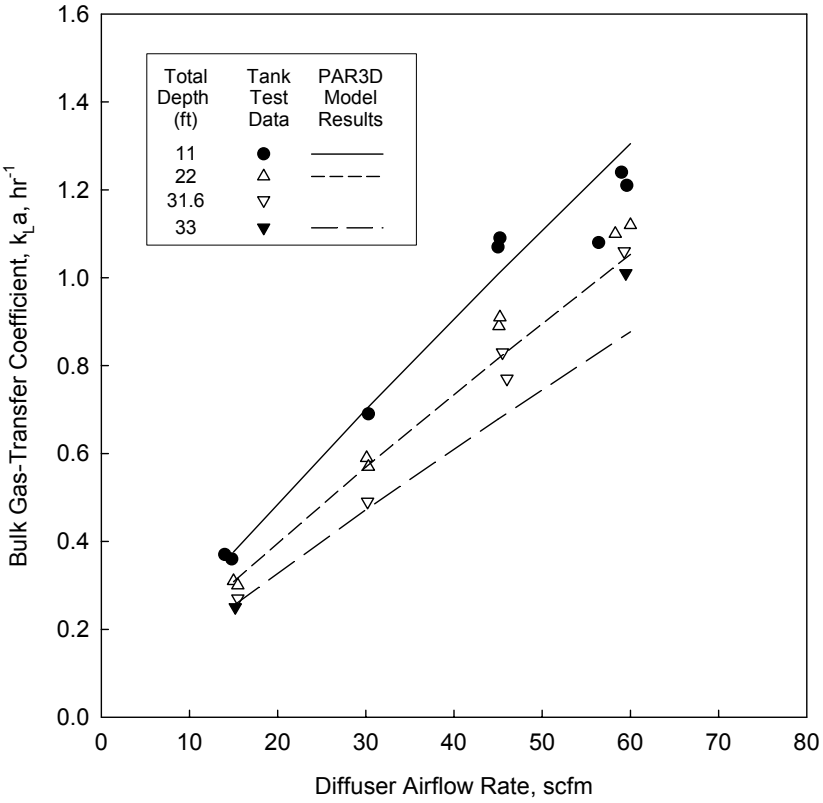

Figure 2. Bulk gas-transfer coefficients for coarse-bubble diffuser submerged in 25-ft-diameter tank

Conclusion

The model application presented here involves only a single diffuser in a cylindrical tank, but PAR3D can also accommodate multiple diffusers and complex geometries. Given these added capabilities, the model offers a convenient means for evaluating the performance of bubble diffusers, either as mixers or aerators (or both), in diverse configurations and reservoir conditions (Bernard 1998). Tank tests may be necessary to establish nominal bubble diameters for the diffusers that are to be modeled, but otherwise PAR3D should require no further (empirical) adjustment by the user.

For applications involving bubble diffusers in particular, the essential model input consists of a computational grid representing the tank or reservoir, along with the locations, airflow rates, and nominal bubble diameters for the diffusers in question. The volume occupied by each diffuser is also required, but this can be adequately represented by using the largest lateral dimension of the actual diffuser as the side (or diameter) of a rectangular (or cylindrical) grid region containing the simulated diffuser.

Concerning accuracy, experience to date (with bubble diffusers) suggests that PAR3D predicts gas-transfer rates reliably within about 20 percent, and time-averaged flow velocities roughly within a factor of two. Future work will examine the accuracy of PAR3D turbulence predictions.

Acknowledgement

The author is grateful for advice and counsel provided by Dr. Steven C. Wilhelms, ERDC Waterways Experiment Station, and Professor John S. Gulliver, University of Minnesota. This work was sponsored by the US Army Engineer District, Chicago. Permission was granted by the Chief of Engineers to publish this information.

References

Bernard, R. S. (1995). "Preliminary development of a three-dimensional numerical model for reservoir hydrodynamics." Technical Report HL-95-9, ERDC Waterways Experiment Station, Vicksburg, MS.

Bernard, R. S. (1998). "MAC3D: Numerical model for reservoir hydrodynamics with application to bubble diffusers." Technical Report CHL-98-23, ERDC Waterways Experiment Station, Vicksburg, MS.

Clift, R., Grace, J. R., and Weber, M. E. (1978). *Bubbles, Drops, and Particles*, Academic Press, New York.

Fortesque, G. E., and Pearson, J. R. A. (1967). "On gas absorption into a turbulent liquid." *Chemical Engineering Science*, 22, 1163.

Launder, B. E., and Spalding, D. B. (1974). "The numerical calculation of turbulent flows." *Computer Methods in Applied Mechanics and Engineering*, 3, 269-289.

Levich, V. G. (1962). *Physicochemical Hydrodynamics*, Prentice-Hall, Englewood Cliffs, NJ.

Rodi, W. (1980). "Turbulence models and their application in hydraulics." State-of-the-Art Paper, International Association for Hydraulic Research, Delft, Netherlands.

Appendix

PAR3D uses a variant of the *k-,* model developed by Launder and Spalding (1974) to account for turbulence in the computed flow. The turbulence energy (per unit mass) is denoted by *k*, and its dissipation rate is denoted by ,. The governing equations for the transport and production of these two quantities are

$$\frac{Dk}{Dt} = P - \varepsilon + \frac{1}{\sigma_k} div\,(\nu_T\ grad\ k)$$

$$\frac{D\varepsilon}{Dt} = \frac{\varepsilon}{k}(c_1 P - c_2 \varepsilon) + \frac{1}{\sigma_\varepsilon} div\,(\nu_T\ grad\ \varepsilon)$$

where the eddy viscosity (previously defined) is denoted by ν_T; and c_1, c_2, Φ_k, and Φ_ε are empirical coefficients. The rate of turbulence-energy production, arising from shear and buoyancy in the computed flow, is given by

$$P = \nu_T \left[2\left(u_x^{\,2} + v_y^{\,2} + w_z^{\,2}\right) + (u_y + v_x)^2 + (u_z + w_x)^2 + (v_z + w_y)^2 + \frac{\rho_z g}{\rho}\right]$$

where ρ is the density; g is gravitational acceleration; u, v, and w are x-, y-, and z-components of velocity; and the subscripts x, y, and z indicate spatial derivatives.

Observing that, for hydrostatic conditions, the pressure p is related to ρ and g by

$$p_z = -\rho_z g$$

one can then replace $\rho_z g$ with $-p_z$ in the previous expression for P. Extending this observation to *non-hydrostatic* conditions in general, it is *assumed* that p_z can be replaced with the Laplacian of pressure in three dimensions,

$$div\,(grad\ p) = p_{xx} + p_{yy} + p_{zz}$$

Accordingly, the generalized expression for the production rate becomes

$$P = \nu_T \left[2\left(u_x^{\,2} + v_y^{\,2} + w_z^{\,2}\right) + (u_y + v_x)^2 + (u_z + w_x)^2 + (v_z + w_y)^2 - \frac{div\,(grad\ p)}{\rho}\right]$$

In the governing equations for k and ε, the empirical coefficients must satisfy the constraint,

$$c_1 - c_2 + \frac{\kappa^2}{\sigma_\varepsilon \sqrt{c_\nu}} = 0$$

where $c_\nu = 0.09$ and κ is von Karman's constant. The recommended (standard) values for these coefficients are $c_1 = 1.44$, $c_2 = 1.92$, $\Phi_k = 1.0$, and $\Phi_\varepsilon = 1.3$, consistent with $\kappa \approx 0.433$.

With the recommended set of values, however, the *k-,* model generally over-predicts turbulence energy in recirculating flow. To counter this tendency somewhat, PAR3D uses $c_1 = 1.59$, $c_2 = 1.92$, $\Phi_k = 1.0$, and $\Phi_{,} = 1.6$, with $6 = 0.4$. Of these, the unaltered value for c_2 comes directly from observed rates of turbulence decay (Rodi 1980), and the value chosen here for 6 lies in the conventional range for von Karman's constant. Apart from Φ_k, whose value is also unaltered, only one of the remaining coefficients (c_1 or $\Phi_{,}$) can be set independently, while the other then follows from the constraint. In particular, the larger values used by PAR3D for c_1 and $\Phi_{,}$ tend to produce greater rates of turbulence dissipation, and lesser turbulence energies, than do the smaller standard values.

To allow for turbulence production that is *not* dominated by boundary influences, PAR3D imposes a symmetry condition for *k* and *,* along slip boundaries (symmetry boundaries), no-slip walls (friction boundaries), and free surfaces alike. This requires only that normal derivatives of *k* and *,* vanish at these boundaries; i.e.,

$$\frac{\partial k}{\partial n} = \frac{\partial \varepsilon}{\partial n} = 0$$

where *n* is the direction normal to the boundary in question.

Along no-slip walls, the kinematic shear stress ϑ_w imposed by the wall alone is computed from the conventional law of the wall, whereby

$$\tau_w = u_*^2$$

and the friction velocity u_* is extracted from a transcendental equation that relates u_* to the tangential velocity *u*, the molecular viscosity <, and the normal distance * from the wall; i.e.,

$$\frac{u}{u_*} = \frac{1}{\kappa} \ln\left(\frac{u_* \delta}{\nu}\right) + C$$

where

$$C \approx 5.5$$

and the value given for *C* is appropriate for a hydraulically smooth wall (Rodi 1980).

Strictly speaking, the law of the wall applies only to a fully developed, turbulent shear flow along a perfectly flat surface. For typical PAR3D gas-transfer applications, however, the grids employed are usually much too coarse to resolve the actual near-wall velocity distribution, and the logarithmic velocity formula merely provides a convenient (but rough) estimate for the friction velocity and the resulting shear stress at the wall. The conventional law of the wall also constrains the turbulence energy to

be $k = c_{<}^{-1/2} u_*^2$ near the wall, but this relation is *not* used in PAR3D applications because turbulence production is generally dominated by processes occurring well away from the walls.